

Experimental Demonstration of Longitudinal Beam Phase-Space Linearizer in a Free-Electron Laser Facility by Corrugated Structures

Haixiao Deng,¹ Meng Zhang,¹ Chao Feng,¹ Tong Zhang,¹ Xingtao Wang,¹ Taihe Lan,¹ Lie Feng,¹ Wenyan Zhang,¹ Xiaoqing Liu,¹ Haifeng Yao,¹ Lei Shen,¹ Bin Li,¹ Junqiang Zhang,¹ Xuan Li,¹ Wencheng Fang,¹ Dan Wang,²

Marie-emmanuelle Couprie,³ Guoqiang Lin,¹ Bo Liu,¹ Qiang Gu,¹ Dong Wang,¹ and Zhentang Zhao^{1,*}

¹Shanghai Institute of Applied Physics, Chinese Academy of Sciences, Shanghai 201800, People's Republic of China

²Department of Engineering Physics, Tsinghua University, Beijing 100084, People's Republic of China

³Synchrotron SOLEIL, L'Orme des Merisiers, Saint-Aubin, BP 48, 91192 Gif-sur-Yvette, France

(Received 1 October 2014; published 19 December 2014)

Removal of the undesired time-energy correlations in the electron beam is of paramount importance for efficient lasing of a high-gain free-electron laser. Recently, it has been theoretically and experimentally demonstrated that the longitudinal wakefield excited by the electrons themselves in a corrugated structure allows for precise control of the electron beam phase space. In this Letter, we report the first utilization of a corrugated structure as a beam linearizer in the operation of a seeded free-electron laser driven by a 140 MeV linear accelerator, where a gain of ~ 10000 over spontaneous emission was achieved at the second harmonic of the 1047 nm seed laser, and a free-electron laser bandwidth narrowing by 50% was observed, in good agreement with the theoretical expectations.

DOI: 10.1103/PhysRevLett.113.254802

PACS numbers: 41.60.Cr

The recent advent of the x-ray free-electron laser (FEL) presenting high brightness, an ultrashort pulse, a tunable wavelength, and flexible polarization pushes nonlinear optics science into the x-ray domain. FELs open new frontiers of ultrafast science in the multidisciplinary investigation of matter and pave the way for various novel time-resolved experiments [1,2]. The FEL generates coherent radiation by wiggling a relativistic electron beam passing through an undulator, with the capability of tuning radiation frequencies from the infrared to hard x-ray regions [3,4]. In order to achieve efficient lasing for outstanding FEL performance, precise control of the electron beam is required, mainly for a high peak current and/or constant energy profile along the longitudinal dimension. In a linear accelerator (LINAC) driven high-gain FEL, the electron beam from the cathode is usually accelerated in radio frequency (rf) cavities and temporally compressed in magnetic chicanes, which leaves an undesired time-energy correlation in the electron bunch, i.e., a linear energy chirp and nonlinear energy curvature [5–8]. Such time-energy correlations are usually detrimental to the FEL performance.

As well illustrated theoretically and experimentally [9–13], with a linear energy chirp of h , the output wavelength of a seeded FEL, e.g., high-gain harmonic generation (HG) [14], will shift to

$$\lambda_{\text{HG}} = \lambda_s(1 + hR_{56})/n, \quad (1)$$

where λ_s is the seed wavelength, R_{56} is the dispersion of the chicane, and n is the harmonic number. Thus, a linear chirp leads to a wavelength shift while a nonlinear one contributes to a bandwidth broadening. Although the

degradations of the FEL spectrum in HG schemes due to the beam energy correlations can be partly cured by advanced seeding concepts, e.g., echo-enabled harmonic generation [15,16] and phase-merging enhanced harmonic generation [17–19], it is preferred that the energy correlations be removed before the FEL process. Typically, the removal of the linear energy chirp is done by cooperation of off-crest acceleration and wakefields induced in downstream accelerator cavities, while the correction of nonlinear rf curvature can be accomplished in a harmonic cavity, shaping the electron beam current at the photoinjector [20], and using sextupoles to control second-order effects in achromatic sections [21,22].

An alternative, rf-free approach to correct the undesired energy correlation in the electron beam is the dedicated structure, which can intentionally generate a strong longitudinal wakefield. The structures suggested for such purposes are a beam pipe with a thin dielectric layer [23], a resistive pipe of small radius [24], and a metallic pipe with periodic corrugations [25]. Currently, the corrugated metallic structure is attracting great interest in the accelerator community, as its wakefield may reach the maximal strength for a given aperture. Moreover, both the frequency and amplitude of the wake can be easily adjusted by choosing the corrugation parameters. Theoretical investigations indicate that corrugated structures can be used to remove the residual linear energy chirp [25], to linearize the high-order rf curvatures [26,27], and to stabilize the beam jitter [28], provided that the electron bunch length and the structure parameters are well matched. Recently, experiments using passive wakefields to remove the linear energy correlation of the electron beam have been

successfully demonstrated with dielectric structures [29,30] and metallic corrugated devices [31,32]. Therefore, it is widely believed that such passive wakefield devices can significantly reduce cost and improve FEL performance, and almost every new FEL facility is seriously considering the idea of using corrugated structures to control the longitudinal phase space of the electron beam [33–36].

So far, the effect of a corrugated structure has only been tested on LINACs as a beam dechirper [31,32]. In this Letter, we report the demonstration of a metallic corrugated structure serving as a beam linearizer in a seeded FEL facility. A FEL bandwidth narrowing by 50% and an obvious FEL central wavelength shift in the experiment confirm the feasibility of employing a corrugated device for the precise control of the electron beam, and thus to improve the output performances in future x-ray FEL user facilities.

The geometry of a corrugated structure is plotted in Fig. 1, which can be manufactured by low-speed wire-cut electrical discharge machining. Usually a rectangular geometry is preferred since it provides operational flexibility and can be effective for different electron bunch cases. The corrugations are characterized by the period p , depth δ , gap g , length l , and width w . According to wakefield theory [25,33,37,38], in the wide structure limit, the longitudinal wakefield generated by an electron passing the corrugated plates is a damped cosine oscillation, which can be numerically fitted as follows:

$$w(z) = \left(\frac{\pi^2}{16}\right) \frac{Z_0 c}{\pi a^2} H(z) F e^{-(k/2)(z/Q)} \cos(kz), \quad (2)$$

where $Z_0 = 377\Omega$ is the impedance of free space, $H(z)$ is the step function, c is the speed of light, z is the coordinate along the beam path, and F , k , and Q are the amplitude factor, wave number, and quality factor, respectively, which are functions of the corrugation parameters [38]. The dominant wave number of the wakefield can be

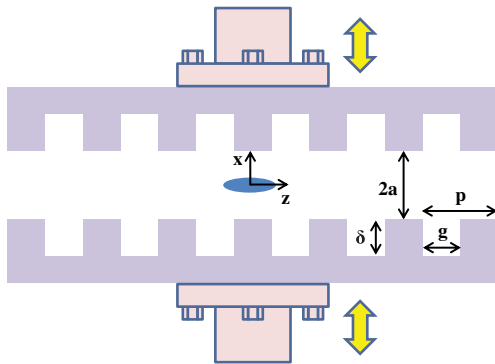


FIG. 1 (color online). Moveable corrugated plates, where a rectangular coordinate system is centered on the axis. For the case in this Letter, the separation between the two aluminum plates can be adjusted from $a = 1$ to 25 mm, with parameters $p = 0.6$ mm, $\delta = 2.0$ mm, and $g = 0.3$ mm, and plate lengths of 0.3 m and plate widths of 30 mm.

approximated as $k = [p/(a\delta g)]^{1/2}$. The wakefield produced by a beam can be found by convolving the wake function with the longitudinal bunch profile. When the induced energy loss along the electron beam is a sinusoidal waveform with a wavelength of about twice the bunch length, it can be used as a linearizer for the temporal phase space.

As shown in Fig. 2, the experiment was conducted in a HGHG-FEL lasing process at the Shanghai deep ultraviolet FEL (SDUV-FEL) facility [39–42]. The LINAC consists of an S-band photoinjector (150 pC bunch charge and 30 MeV beam energy), and four S-band accelerating modules (A1–A4) symmetrically placed on both sides of the magnetic compressor. The LINAC provides 140 MeV beams, with a normalized emittance of 4 μm rad, a global energy spread of 0.1%, and a pulse duration of 8.8 ps (FWHM) without compression. The seed of the HGHG FEL is a 1047 nm laser with a pulse length of 8.7 ps (FWHM) and a tunable pulse energy up to 100 μJ . The beam energy modulation is achieved when the electron beam and laser overlap spatially and temporally in the short electromagnetic undulator (i.e., modulator after UNPRF0, ten periods with a period of 65 mm) and, afterwards, the electron beam passes through a dispersive chicane with R_{56} of 0–70 mm, to form the density modulation, where the phase and amplitude properties of the seed pulse are encoded into the electrons. Finally, the microbunched electron beam is sent through the radiator sections, which comprise two segments of the 1.6 m long undulator with a period of 40 mm, to produce coherent FEL radiation at the second harmonic of the seed laser. Considering the requirement for the beam phase space linearization and the free space available at the SDUV-FEL, a pair of corrugated plates wrapped in a 0.5 m vacuum chamber was equipped after the modulator. The chamber support includes two separate motors to allow for independent positioning for each corrugated jaw, providing remote control of the full horizontal separation with a 4 μm resolution, as well as the horizontal central position.

For predicting the FEL performance dependence on the corrugated wakefield linearizer, we carried out self-consistent 3D simulations [43] in which all macroparticles are directly tracked from the photocathode to the undulator exit by using a set of well-benchmarked codes. First, the macroparticles are tracked by ASTRA [44] in the photoinjector. Then, the 6D phase space is further tracked by ELEGANT [45] for the energy booster. The electron's behavior in the modulator is determined by the magnetic field and the laser electric field in the time domain [46]. The pass through the corrugated chambers is implemented in ELEGANT, where the corrugated plate is replaced by a pipe with an equivalent longitudinal wakefield. After the particle dumping from ELEGANT, the bunch is loaded into GENESIS [47] for FEL simulation.

Three cases with the accelerating phase of A3 and A4 being 0° , -25° , and 25° are considered here, as illustrated

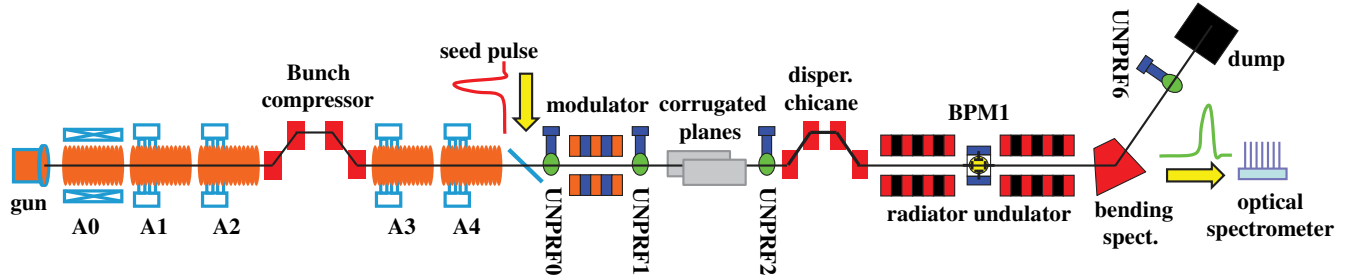


FIG. 2 (color online). Schematic layout of experiment at the SDUV-FEL. In the experiment, two correctors attached at the two edges of the modulator are first fine tuned for beam trajectory control in the corrugated structures, while the signals from UNPRF2 and BPM1 serve as the reference monitor of the bunch charge, thus to make sure that the electron beam passes through the corrugated chamber without much loss. Then, screens UNPRF0 and UNPRF1 are used to spatially synchronize the electron and laser in the modulator. The FEL radiation properties were investigated with a spectrometer, a photodetector, and a charge-coupled device.

by the simulation results in Fig. 3. In the case of the on-crest acceleration shown in Fig. 3(a), the projected beam energy spread can be significantly suppressed by a factor of about 50%, while in the two off-crest acceleration cases shown in Figs. 3(b) and 3(c), the nonlinear beam energy correlations induced by the rf curvature were corrected by the wakefield of the corrugated plates. It is worth stressing that, for a seeded FEL configuration under such a linearization, besides a FEL bandwidth reduction, a FEL central wavelength shift may also be induced, depending on the beam energy chirp variation at the core of the electron beam.

The corrugated structure experiments at the SDUV-FEL were performed at the second harmonic of the laser seeding, and the accelerating phases of A3 and A4 were 25° ; thus, the beam energy correlations shown in Fig. 3(c) were expected before and after the linearization. In order to clearly distinguish the corrugated plate effects from the machine instabilities, a relatively large dispersion of $R_{56} = 6.5$ mm was used. FEL simulations were carried out under the experimental conditions. As the simulated results show in Fig. 4(a), a linear energy chirp of $h \approx 7.8$ m $^{-1}$ leads to an output central wavelength shift from 523 to 550 nm for the case without beam linearization. The central wavelength is further shifted to 558 nm with an appropriate linearization.

Simultaneously, the FEL bandwidth broadening due to the nonlinear rf curvature is significantly compensated by the wakefield. In the experiment, the seed laser was first optimized in the modulator to achieve maximum FEL radiation. At this stage, the two corrugated plates were opened ($a = 3.0$ mm) and a 550 nm HGHG signal with a 7.8 nm bandwidth was observed [see the blue line in Fig. 4(b)]. Then, the two corrugated plates were gradually closed to compensate the nonlinear rf curvature, which led to a wavelength shifting and a bandwidth narrowing of the HGHG output. When the corrugated plates were in their optimized gap ($a = 1.0$ mm), the HGHG spectrum located at 558 nm [Fig. 4(b), red line] with an intensity relatively larger than that before the correction, and a spectral bandwidth of 3.7 nm, was generated. To show the repeatability of the measurements, eight consecutive radiation spectra observed from experiment are illustrated in Fig. 4(c). The HGHG bandwidth without beam linearization, averaged over eight shots, is found to be 7.34 ± 0.47 nm while that for the appropriate linearization case is only 3.75 ± 0.26 nm. The experiments agree well with the simulations.

Considering that the FEL spectrum would be amplified and purified further during the exponential growth process in the radiator, in order to illustrate the electron beam energy correlation, the FEL lasing here was accomplished

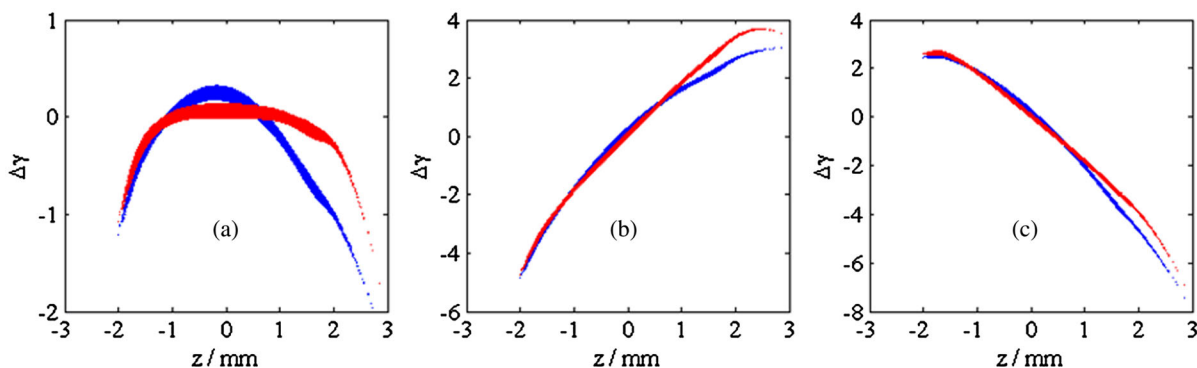


FIG. 3 (color online). Simulated phase space of the electron beam, where the blue and red lines represent the phase space before and after the corrugated device, respectively, with the phases of A3 and A4 being (a) 0° , (b) -25° , and (c) 25° .

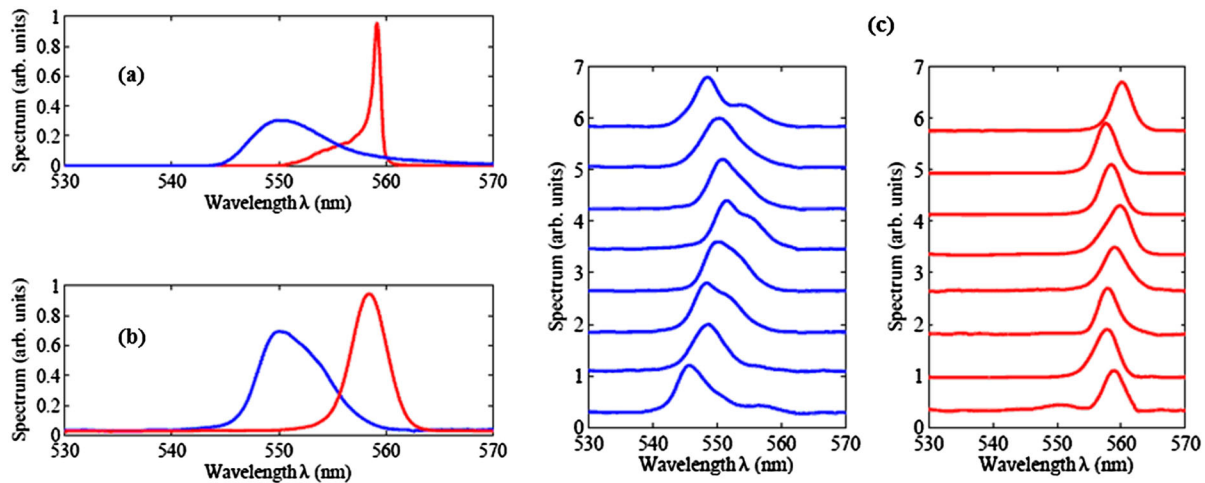


FIG. 4 (color online). FEL spectra from the simulation and experiment for two corrugated plane gaps (red at $a = 1.0$ mm and blue at $a = 3.0$ mm). (a) Simulated radiation spectra. (b) Typical spectra from experiment. The measurements were performed with a commercial spectrometer (model TRIAX-550, Jobin Yvon) with a focal length of 550 mm, a grating of 600 lines/mm, and a calibrated resolution of 2.7 nm with the front slit open. (c) Sequence of eight consecutive shots of FEL spectra from experiment.

without any beam compression, i.e., with a lower FEL gain. The FEL pulse energy was measured with SXUV100 photodetectors (International Radiation Detectors) and homemade amplifiers. The efficiency was calibrated with a pulsed laser with an uncertainty of 30%. Under such circumstances, the measured FEL pulse energies are almost similar in the experiments with and without the corrugated structure linearizer, i.e., ~ 200 nJ. It indicates that a FEL gain larger than 1×10^4 is achieved compared with the spontaneous radiation from one segment radiator. Therefore, by an $\sim 50\%$ FEL bandwidth decrease and FEL gain hold, the FEL brightness is estimated to be about 100% higher with the corrugated linearizer, which is in reasonable agreement with numerical simulation.

Moreover, a 30° bending spectrometer with the screen UNPRF6 (a 300-kpx camera with a $7.5 \mu\text{m}/\text{pixel}$ resolution) located downstream of the undulators is used for the beam energy distribution measurement. Under the on-crest acceleration situation, a selection of beam energy spectrum measurements at different plate separations was carried out to verify the energy spread suppression by corrugated wakefield compensation. Figure 5 shows the measured energy distribution of the electrons with various wakefield strengths. The relative electron beam energy spread was suppressed from 1.1×10^{-3} to 7.5×10^{-4} , which is quite consistent with the beam tracking results, if one considers the contribution of the horizontal beam size.

In summary, we experimentally demonstrated the possibility of linearizing the beam energy curvature imprinted by the rf field during beam acceleration, by using a twin plane with metallic corrugations, in a laser seeding HGHG-FEL configuration at the Shanghai deep ultraviolet FEL facility. By closing the corrugated linearizer separation from 6.0 to 2.0 mm, the initial FEL bandwidth of 7.34 nm was gradually reduced to 3.75 nm, together with an

approximate 8.0 nm redshift of the FEL central wavelength. The residual bandwidth corresponded to the imperfection of the 1047 nm seed laser, not a fully optimized experimental condition, and mainly to the limited spectrometer resolution of 2.7 nm. Reasonably good agreement between the measurement and the model is observed, and our results give one confidence that the corrugated structure can in practice significantly simplify LINAC design and improve the performance of FELs, especially in seeded FELs in pursuit of fully coherence.

This technique can be extended to advanced single-shot MeV transmission electron microscopy [48,49], where a low energy spread is very critical to minimize spherical and chromatic aberrations and reach a 10 nm spatial resolution. If one considers the small beam size in transmission

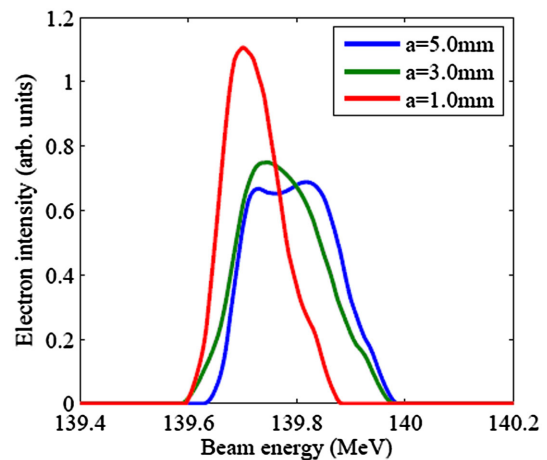


FIG. 5 (color online). The beam energy distribution measurement with on-crest acceleration of A3 and A4 cavities, in which the corrugated linearizer with the separation parameter $a = 5.0$, 3.0, and 1.0 mm, respectively, was used.

electron microscopy, a tunable corrugated linearizer is a promising choice for compensating the beam energy spread, and no additional instability is expected in such a passive linearizer.

The authors thank the SDUV-FEL staff for excellent support during the experiment. They also thank D. Xiang, Z. Huang, and G. Stupakov for their helpful discussions. This work was partially supported by the Ministry of Science and Technology of China (Grant No. 2011CB808300) and the National Natural Science Foundation of China (Grants No. 11175240, No. 11205234, No. 11322550, and No. 11475250).

* zhaozhentang@sinap.ac.cn

- [1] H. N. Chapman, P. Fromme, A. Barty *et al.*, *Nature (London)* **470**, 73 (2011).
- [2] A. Barty, J. Kopper, and H. N. Chapman, *Annu. Rev. Phys. Chem.* **64**, 415 (2013).
- [3] J. Madey, *J. Appl. Phys.* **42**, 1906 (1971).
- [4] B. W. J. McNeil and N. R. Thompson, *Nat. Photonics* **4**, 814 (2010).
- [5] J. Arthur *et al.*, Stanford Report No. SLAC-R-593, 2002.
- [6] P. Emma, R. Akre, J. Arthur *et al.*, *Nat. Photonics* **4**, 641 (2010).
- [7] E. Allaria, R. Appio, L. Badano *et al.*, *Nat. Photonics* **6**, 699 (2012).
- [8] T. Ishikawa, H. Aoyagi, T. Asaka *et al.*, *Nat. Photonics* **6**, 540 (2012).
- [9] T. Shaftan and L. H. Yu, *Phys. Rev. E* **71**, 046501 (2005).
- [10] Z. Huang *et al.*, in *Proceedings of the 2009 Free-Electron Laser Conference, Liverpool, UK, 2009*, p. 221.
- [11] D. Xiang *et al.*, *Phys. Rev. Lett.* **105**, 114801 (2010).
- [12] Z. Zhao *et al.*, *Nat. Photonics* **6**, 360 (2012).
- [13] G. Wang, C. Feng, H. Deng, T. Zhang, and D. Wang, *Nucl. Instrum. Methods Phys. Res., Sect. A* **753**, 56 (2014).
- [14] L. H. Yu, *Phys. Rev. A* **44**, 5178 (1991).
- [15] G. Stupakov, *Phys. Rev. Lett.* **102**, 074801 (2009).
- [16] E. Hemsing, M. Dunning, C. Hast, T. O. Raubenheimer, S. Weathersby, and D. Xiang, *Phys. Rev. ST Accel. Beams* **17**, 070702 (2014).
- [17] H. Deng and C. Feng, *Phys. Rev. Lett.* **111**, 084801 (2013).
- [18] C. Feng, H. Deng, D. Wang, and Z. Zhao, *New J. Phys.* **16**, 043021 (2014).
- [19] C. Feng, T. Zhang, H. Deng, and Z. Zhao, *Phys. Rev. ST Accel. Beams* **17**, 070701 (2014).
- [20] G. Penco, M. Danailov, A. Demidovich, E. Allaria, G. De Nino, S. Di Mitri, W. M. Fawley, E. Ferrari, L. Giannessi, and M. Trovó, *Phys. Rev. Lett.* **112**, 044801 (2014).
- [21] R. J. England, J. Rosenzweig, G. Andonian, P. Musumeci, G. Travish, and R. Yoder, *Phys. Rev. ST Accel. Beams* **8**, 012801 (2005).
- [22] S. Thorin *et al.*, in *Proceedings of the 2014 Linear Accelerator Conference, Geneva, Switzerland, 2014* (unpublished).
- [23] M. Rosing and J. Simpson, Report No. ANL Report WF-144, 1990.
- [24] H. Kang, J. Han *et al.*, in *Proceedings of the 2012 Free-Electron Laser Conference, Nara, Japan, 2012*, p. 309.
- [25] K. Bane and G. Stupakov, *Nucl. Instrum. Methods Phys. Res., Sect. A* **690**, 106 (2012).
- [26] P. Craievich, *Phys. Rev. ST Accel. Beams* **13**, 034401 (2010).
- [27] Q. Gu, M. Zhang, and M. Zhao, in *Proceedings of the 2012 Linear Accelerator Conference, Tel-Aviv, Israel, 2012*, 525.
- [28] M. Zhang, X. Li, H. Deng, and Q. Gu, *High Power Laser Part. Beams* **26**, 015106 (2014).
- [29] S. Antipov, C. Jing, M. Fedurin, W. Gai, A. Kanareykin, K. Kusche, P. Schoessow, V. Yakimenko, and A. Zholents, *Phys. Rev. Lett.* **108**, 144801 (2012).
- [30] S. Antipov, S. Baturin, C. Jing, M. Fedurin, A. Kanareykin, C. Swinson, P. Schoessow, W. Gai, and A. Zholents, *Phys. Rev. Lett.* **112**, 114801 (2014).
- [31] P. Emma *et al.*, *Phys. Rev. Lett.* **112**, 034801 (2014).
- [32] M. Harrison *et al.*, in *Proceedings of the 2013 North American Particle Accelerator Conference, Pasadena, USA, 2013*, p. 291.
- [33] K. Bane and G. Stupakov, Report No. SLAC-PUB-15852, 2013.
- [34] K. Bane, P. Emma *et al.*, Report No. SLAC-PUB-15853, 2013.
- [35] S. Bettoni, P. Craievich *et al.*, in *Proceedings of the 2013 Free-Electron Laser Conference, New York, USA, 2013*, p. 214.
- [36] M. Harrison *et al.*, in *Proceedings of the 2014 Free-Electron Laser Conference, Basel, Switzerland, 2014* (unpublished).
- [37] K. L. F. Bane and G. Stupakov, *Phys. Rev. ST Accel. Beams* **6**, 024401 (2003).
- [38] Z. Zhang *et al.*, in *Proceedings of the 2014 Free-Electron Laser Conference, Basel, Switzerland, 2014* (unpublished).
- [39] Z. Zhao, Z. M. Dai, X. F. Zhao, D. K. Liu, Q. G. Zhou, D. H. He, Q. K. Jia, S. Y. Chen *et al.*, *Nucl. Instrum. Methods Phys. Res., Sect. A* **528**, 591 (2004).
- [40] B. Liu *et al.*, *Phys. Rev. ST Accel. Beams* **16**, 020704 (2013).
- [41] H. Deng *et al.*, *Phys. Rev. ST Accel. Beams* **17**, 020704 (2014).
- [42] H. Deng, *Nucl. Sci. Tech.* **25**, 010101 (2014).
- [43] J. Yan, M. Zhang, and H. Deng, *Nucl. Instrum. Methods Phys. Res., Sect. A* **615**, 249 (2010).
- [44] K. Flottmann, ASTRA User Manual, <http://www.desy.de/~mpyflo>.
- [45] M. Borland, ANL Advanced Photon Source, Report No. LS-287, 2000.
- [46] H. Deng, Tang-Yu Lin, J. Yan, D. Wang, and Zhi-Min Dai, *Chin. Phys. C* **35**, 308 (2011).
- [47] S. Reiche, *Nucl. Instrum. Methods Phys. Res., Sect. A* **429**, 243 (1999).
- [48] R. K. Li and P. Musumeci, *Phys. Rev. Applied* **2**, 024003 (2014).
- [49] D. Xiang, F. Fu, J. Zhang, X. Huang, L. Wang, X. Wang, and W. Wan, *Nucl. Instrum. Methods Phys. Res., Sect. A* **759**, 74 (2014).